CHAPTER 13

ESTABLISHING CLIMATE DATA RECORDS FROM MULTISPECTRAL MODIS MEASUREMENTS

13.1 The MODIS Spectral Bands

The Moderate Resolution Imaging Spectroradiometer (MODIS) is an Earth Observing System (EOS) facility instrument that is currently flying aboard the Terra and Aqua spacecraft. It is especially well suited to global monitoring of atmospheric properties from space, and is based on heritage sensors such as the Advanced Very High Resolution Radiometer (AVHRR), Landsat Thematic Mapper (TM), High-resolution Infrared Radiation Sounder (HIRS), and the Nimbus-7 Coastal Zone Color Scanner (CZCS). The MODIS is a scanning spectro-radiometer with 36 spectral bands between 0.645 and 14.235 μm (King et al. 1992). Table 13.1 lists the MODIS spectral channels and their primary application. Bands 1 - 2 are sensed with a spatial resolution of 250 m, bands 3 - 7 at 500 m, and the remaining bands 8 – 36 at 1000 m. The signal to noise ratio in the reflective bands ranges from 50 to 1000; the noise equivalent temperature difference in the emissive bands ranges from 0.1 to 0.5 K (larger at longer wavelengths). Figure 13.1 shows the spectral bands superimposed on the earth reflection and emission spectra.

13.2 Climate Questions

13.2.1 Energy Balance

The flow of radiation from the Sun to the Earth, its absorption, reflection, and emission, determines the energy balance of the Earth, and hence the nature of the life of its inhabitants. The information from products describing optical and physical properties of clouds and aerosols is combined with broadband radiation measurements to provide estimates of solar and infrared radiative fluxes, which, in turn, determine the heating and cooling of the Earth and the atmosphere. The necessary radiation estimates are shortwave and longwave fluxes at the surface and top of the atmosphere, both downwelling and upwelling, so that the net flow can be determined. Fluxes must be distinguished between cloudy and clear-sky regions as the flow of energy to and from the Earth is modulated by clouds and aerosols. Measuring and understanding these elements is key to predicting climate change and to testing global climate models. The technology for accurately measuring radiative fluxes, cloud properties, and aerosol properties from space has advanced to the point that these observations can be used to greatly advance our ability to address critical global change issues. For example, if the global climate changes, do clouds generate a positive or negative feedback? Do aerosols offset some of the expected warming due to the increase in greenhouse gases? Figure 13.2 indicates the annual mean global energy balance for the earth-atmosphere system. Tracking the global energy balance trends is a vital part of climate change research.

Clouds: A key step in measuring cloud properties from space is to determine where clouds exist, how they are distributed through the atmosphere, and what their dimensions are. Once clouds are identified and mapped, cloud properties, such as effective particle size, thermodynamic phase (water, ice), cloud top properties, and optical thickness (which all help determine how much radiation passes through them), may be measured. These cloud properties help to determine how much solar radiation reaches the Earth and how much escapes back to space. They also supply information on factors that influence cloud formation and forces driving circulation and global climate. Cloud detection and delineation produces masks indicating where clouds exist and information on layering and overlap to give a geometric picture of global cloud coverage. Cloud property retrieval quantifies the physics of the cloud through parameters such as optical thickness, temperature, liquid water content, ice water content, particle radius, cloud top altitude, and phase, which all relate to the radiative transmission, reflection, and emission of the cloud. A thorough

description of global cloudiness and its associated properties is essential because (a) clouds play a critical role in the radiative balance of the Earth and must be accurately described in order to assess climate and potential climate change accurately and (b) the presence or absence of clouds must be accurately determined in order to retrieve properly many atmospheric and surface parameters where often even thin cirrus represents contamination.

Aerosols: The measurement of aerosols, suspended particles in the atmosphere (e.g., dust, sulfate, smoke, etc.), is an important element in describing energy transmission through the atmosphere. Aerosols are a significant source of uncertainty in climate modeling because they affect cloud microphysics by acting as condensation nuclei, thereby affecting cloud radiative properties, the hydrological cycle and atmospheric dynamics. They also interact directly with solar radiation, thus affecting the radiative balance. The location of anthropogenic aerosols is also an important consideration in their impact on climate.

The *Radiant Energy Flux* is an estimate of the radiative flux downward and upward at the top-of-atmosphere, at the Earth's surface, and at selected intermediate altitudes, as well as the net flux, which is used to determine the radiation budget. This budget determines the overall heating and cooling of the atmosphere and Earth's surface and subsequent changes in climate.

13.2.2 The Water Cycle

The hydrological cycle is one of three key Earth system processes that are components of global climate; along with the carbon and energy cycles. Monitoring precipitation and atmospheric humidity is critical to obtaining hydrological-cycle parameters needed for developing global climate models and detecting climate change. The processes that generate rainfall are central to the dynamical, biological, and chemical processes in the atmosphere, in the oceans, and on the land surfaces. Space-based measurements give a more accurate global documentation of tropical rainfall.

The principal research objective is to explore the connection between weather processes and climate change and the fast dynamical/physical processes that govern climate responses and feedbacks. Particularly significant is the transformation of water among its three physical states - vapor, liquid, and solid - in the atmosphere and at the surface of the Earth. The condensation of water in cloud and snow control both the albedo and radiation balance of the planet, and the constant renewal of fresh water resources. The development of weather systems and the associated cloud life cycles play a key role in the water and atmospheric energy. A central science objective is exploring the responses of hydrologic regimes to changes in climate (precipitation, evaporation, and surface run-off) and the influence of surface hydrology (soil moisture, snow accumulation and soil freezing) on climate. Figure 13.3 gives a schematic of the motions associated with individual water molecules between the oceans, water vapor in the atmosphere, water and ice on the land, and underground water.

Precipitation: The majority of global precipitation occurs in the tropics, between latitudes of 30°N and 30°S. Tropical rain is one of the key parameters that affects the global heat balance and the global water cycle. To understand and predict large variations in weather and climate, it is critical to understand the coupling between the atmosphere and the surface below, which is approximately 29% land and 71% ocean. Atmospheric circulation transports both energy and water, moving heat from the tropics to the polar regions. Water that has evaporated from the oceans and the land surface falls as rain or snow, often in places far removed from its point of origin. There is evidence that tropical rainfall variability, apparently coupled with changes in the underlying surface (particularly sea surface temperature), is associated with significant alterations in wind patterns and rainfall. Fluctuations in rainfall amount impact climate on both short and long time scales. Unlike the small-scale general features that appear on daily weather maps, the long-term, time-averaged circulation and precipitation fields show large-scale features associated with the annual evolution of the monsoons, trade wind systems, and oceanic convergence zones. Large-scale features are also evident on a monthly and seasonal scale. Inter-annual variability is dominated by tropical Pacific ocean-atmosphere interactions. These interactions are associated with the El Niño-Southern

Oscillation (ENSO) cycle, whose major swings, which occur at irregular intervals of two to seven years, are associated with pronounced year-to-year precipitation variations over large areas of the tropics. The large-scale spatial coherence and systematic evolution of both intra-seasonal and inter-annual tropical precipitation anomalies is of great significance to climate prediction. They are also important in the development of optimal sampling strategies for estimating accumulated precipitation over periods of a few weeks to a few months. The characterization of rainfall in tropical regimes is fundamental to improving techniques of radar-rainfall measurements as well. Not only are there regional and seasonal differences, but significant differences also occur within tropical rain systems. These differences can be broadly classified as 1) morphological, referring to sizes, lifetimes, and spatial structures of rain-producing systems; and 2) microphysical, referring to raindrop formation processes, and the raindrop size distribution. Rainfall rates display a highly variable structure in both time and space, meaning radar surveillance systems must take frequent measurements to accurately assess rainfall totals. Three dimensional volume scans (like the WSR-88D radar scans on the nightly weather reports) every five minutes are desirable, although scans at 15-minute intervals provide useful data. The hydrological and severe weather monitoring requirements of most operational radar systems satisfy these criteria, providing invaluable ground-based validation data with nominal additional expenditure.

Humidity: Atmospheric circulation redistributes moisture and heat. Water vapor evaporates from the ocean and land surfaces, and is transported to other parts of the atmosphere where condensation occurs, clouds form, and precipitation ensues. There is a net outflow of atmospheric moisture from the tropics, where sea-surface temperatures are high and the warm atmosphere can hold large amounts of water vapor, to higher latitudes, where condensation and precipitation remove the moisture. Current numerical weather prediction models give inconsistent results about the future distribution of precipitation. Humidity is the amount of water vapor in the atmosphere. Water vapor concentration depends on temperature, which determines the total amount of water that the atmosphere can hold without saturation. Hence, water vapor amounts decrease from Equator to Pole and with increasing altitude. Generally, water amounts are less over the continents than over the oceans, and the upper atmosphere is drier than the near-surface atmosphere. Superimposed on this general behavior are smaller variations of water vapor amounts that determine the formation and properties of clouds and rainfall.

13.2.3 The Carbon Cycle

In addition to the natural fluxes of carbon through the Earth system, anthropogenic (human) activities, particularly fossil fuel burning and deforestation, are also releasing carbon dioxide into the atmosphere. When we mine coal and extract oil from the Earth's crust, and then burn these fossil fuels for transportation, heating, cooking, electricity, and manufacturing, we are effectively moving carbon more rapidly into the atmosphere than is being removed naturally through the sedimentation of carbon, ultimately causing atmospheric carbon dioxide concentrations to increase. Also, by clearing forests to support agriculture, we are transferring carbon from living biomass into the atmosphere (dry wood is about 50 percent carbon). The result is that humans are adding ever-increasing amounts of extra carbon dioxide into the atmosphere. Because of this, atmospheric carbon dioxide concentrations are higher today than they have been over the last half-million years or longer.

Not all of the carbon dioxide that has been emitted by human activities remains in the atmosphere. The oceans have absorbed some of it because as the carbon dioxide in the atmosphere increases it drives diffusion of carbon dioxide into the oceans. However, when we try to account for sources and sinks for carbon dioxide in the atmosphere we uncover some mysteries. For example, notice in Figure 13.4 (schematic of the carbon cycle) that fossil fuel burning releases roughly 5.5 gigatons of carbon (GtC [giga=1 billion]) per year into the atmosphere and that land-use changes such as deforestation contribute roughly 1.6 GtC per year. Measurements of atmospheric carbon dioxide levels (going on since 1957) suggest that of the approximate total amount of 7.1 GtC released per year by human activities, approximately 3.2 GtC remain in the atmosphere, resulting in an increase

in atmospheric carbon dioxide. In addition, approximately 2 GtC diffuses into the world's oceans, thus leaving 1.9 GtC unaccounted for.

What happens to the leftover 1.9 GtC? Scientists don't know for sure, but evidence points to the land surface. However, at this time, scientists do not agree on which processes dominate, or in what regions of the Earth this missing carbon flux occurs. Several scenarios could cause the land to take up more carbon dioxide than is released each year. For example, re-growth of forests since the massive deforestation in the Northern Hemisphere over the last century could account for some of the missing carbon while changing climate could also contribute to greater uptake than release. The missing carbon problem illustrates the complexity of biogeochemical cycles, especially those in which living organisms play an important role. It is critically important that we understand the processes that control these sources and sinks so that we can predict their behavior in the future. Will these sinks continue to help soak up the carbon dioxide that we are producing? Or will they stop or even reverse and aggravate the atmospheric increases? With the use of satellites and field studies, scientists will help to obtain crucial information on the carbon cycle.

13.3 MODIS Product Descriptions

MODIS products are indicated in Table 13.2. The MODIS spectral bands have been chosen to be sensitive to various reflection, absorption, and scattering spectral signatures. Figures 13.5a-d show some of these features. Figure 13.6 shows the processing schema used for deriving atmospheric products from level 0 (raw instrument data) to level 1 (calibrated earth located radiances) to level 2 (5x5 field of view derived atmospheric products) to level 3 (time composited global product fields in even interval lat-lon grid boxes). The following sections outline some of the considerations necessary when deriving some of these products.

13.3.1 Cloud Mask

Cloud measurements are important because clouds often obscure the Earth's surface, complicating measurements of land surface conditions such as vegetative cover or sea surface temperature. At the time of any individual satellite overpass, the Earth scene below MODIS may be covered with clouds. However, the exact same areas aren't likely to be cloudy every day, and scientists can combine, or composite, data over many days to produce weekly and monthly cloud-cleared products that can be used as input to global change models. MODIS's cloud-detection capability is so sensitive that it can even detect clouds that are indistinguishable to the human eye.

The MODIS cloud mask (MOD35) is a global product that provides a probability that a view of the Earth is obstructed by cloud and whether cloud shadow is detected. It also provides information on the processing path taken by the algorithm (land/sea, day/night, etc.), along with individual spectral test results used in the determination of the final cloud mask product. Cloud physical properties are obtained using a set of algorithms operating on multispectral imagery data from multiple sources. Cloud property parameters include particle size and phase, optical thickness, cloud top height, emissivity and temperature, and cloud fraction in a region, all of which support specific MODIS science tasks that complement the radiation studies and products from other instruments.

By using many bands in the visible, near-infrared, and infrared portions of the spectrum at 1-km resolution, improved discrimination between clear and cloudy sky conditions is possible (Ackerman et al., 1998). The reflective bands are used for several cloud tests: (a) reflectance 3.9 μm threshold test; (b) reflectance 1.38 μm threshold indicates presence of thin cirrus cloud; (c) reflectance vegetation ratio test with 0.87 over 0.66 μm; and (d) snow test using 0.55 and 1.6 μm. The emissive bands are used as follows: (a) IR window brightness temperature threshold and difference tests using 8.6, 11, and 12 μm radiances which are sensitive to surface emissivity, atmospheric moisture, dust, and aerosols; and (b) CO2 channel 13.9 micron test for high clouds (available on MODIS only). Figure 13.7 shows the global composite of the average clear-sky MODIS band 31 (11 μm) brightness temperature after filtering out cloud scenes with the cloud mask. The image represents

the average values at 25-km resolution for 5-8 September 2000. Composite images like these have been used extensively in the quality assurance and algorithm adjustment of the cloud mask.

Multispectral investigation of a scene can separate cloud and clear scenes into various classes. Cloud and snow appear very similar in a 0.645 μm image, but dissimilar in a 1.6 μm image (snow reflects less at 1.6 than 0.645 μm). For 8.6 μm ice/water particle absorption is minimal, while atmospheric water vapor absorption is moderate. For 11 μm, the opposite is true. Using these two bands in tandem, cloud properties can be distinguished. Large positive brightness temperature (BT) differences in 8 minus 11 microns indicate the presence of cirrus clouds; negative differences indicate low water clouds or clear skies. Cloud boundaries are often evident in local standard deviation of radiances. Figure 13.8 presents the scatter plots of several bands, LSD, and BT differences versus 11 μm BT for MODIS data collected over the eastern United States on 17 December 2000. Snow and cloud are separated by 1.6 μm, while low and higher clouds are distinguished by 8.6-11 μm BT.

13.3.2 Cloud Properties

Clouds and water vapor play a changing role in radiative forcing, alternatively warming and cooling the Earth. Heavy cloud cover during the day shields the surface from incoming solar energy, cooling the Earth. At night, clouds trap outgoing radiation, warming the Earth. Will increasing global temperatures result in increased evaporation and cloudiness, ultimately cooling the Earth by reflecting solar energy? Or will water vapor's heat-trapping effect outweigh the cooling? Unraveling such complex cause-and-effect relationships, called feedback loops, requires precise measurements of cloud properties: area of coverage, droplet size, cloud-top altitude and temperature, and liquid water content. MODIS near-daily global coverage combined with high spatial and spectral resolution will vastly improve scientists' understanding of clouds.

The MODIS Cloud Product (MOD06) combines infrared and visible techniques to determine both physical and radiative cloud properties. Daily global Level 2 (MOD06) data are provided. Cloud-particle phase (ice vs. water, clouds vs. snow), effective cloud particle radius, and cloud optical thickness are derived using the MODIS visible and near-infrared channel radiances. Cloud-top temperature, height, effective emissivity, phase (ice vs. water, opaque vs. non-opaque), and cloud fraction are produced by the infrared retrieval methods both day and night at 5 x 5 1-km-pixel resolution. Finally, the MODIS Cloud Product includes the cirrus reflectance in the visible at the 1-km-pixel resolution, which is useful for removing cirrus scattering effects from the land-surface reflectance product.

The determination of cloud-top properties requires the use of MODIS bands 29 and 31-36, along with the cloud-mask product (MOD35), to screen for clouds. In addition, NCEP or Data Assimilation Office global model analyses of surface temperature and pressure, profiles of temperature and moisture, and blended SST analyses are required in the calculation of cloud forcing as a function of atmospheric pressure and emissivity.

The technique to infer cloud-top pressure and effective cloud amount (the cloud fraction multiplied by the emittance at 11 μm) has been discussed in detail by Menzel et al. [1983] and Wylie and Menzel [1999]. Error analyses for the method are provided in Wielicki and Coakley [1981], Menzel et al. [1992], and Baum and Wielicki [1994]. The CO_2 slicing method has been used in operational processing of GOES (Geostationary Operational Environmental Satellite) and HIRS (High resolution Infrared Radiometer Sounder) data, and has been found to have accuracies of approximately 50 hPa for clouds at heights above 3 km (approximately 700 hPa). The CO2 radiance measurements have a higher sensitivity to semi-transparent cirrus clouds than visible and infrared window measurements; the threshold for detection appears to be IR optical depths greater than 0.05. The cloud height accuracy increases as the observed cloud signal (the clear sky minus the measured radiance) for a field of view increases; when this difference is near the instrument noise, the infrared window 11-μm band temperature is used to determine a cloud top pressure assuming the cloud is optically thick.

With the four MODIS sounding channels and the 11-μm window band, it is possible to determine a number of separate cloud top pressures and effective cloud amounts. In MODIS operational processing, cloud top pressures are calculated for the following ratio pairs: 14.2 μm/13.9μm; 13.9μm /13.6μm, 13.6μm /13.3μm, 13.9μm /13.3μm, and 13.3μm /11μm. The emission and absorption of the cloud are assumed to be identical in the spectral band pairs. Previous studies have not included the 13.3μm /11μm band pair, but its use is restricted to ice cloud only. The most representative cloud pressure is chosen by minimizing the difference between the observed cloud signal and the cloud signal calculated from a forward radiative transfer model [Menzel et al., 1983]. Figure 13.9 shows the high cloud cover for October 2001 inferred from the MODIS CO2 sensitive bands between 11 and 14.2 microns.

The basis for the inference of cloud phase from the 8.5- and 11-μm bands is the difference of microphysical and optical properties between water droplets and ice crystals [Strabala et al. 1993; Baum et al. 2000b]. Radiative transfer simulations [following Baum et al. 2000a,b] indicate that the brightness temperature difference between the 8.5- and 11-μm bands (hereafter denoted as BTD[8.5-11]) tends to be positive for ice clouds that have an visible optical thickness greater than approximately 1. Water clouds of relatively high optical thickness tend to exhibit highly negative BTD[8.5-11] values of less than -2K. The calculations performed showed that the BTD[8.5-11] values are quite sensitive to atmospheric absorption, especially by water vapor. The BTD value for lower clouds tends to become more negative as the water vapor loading increases, and also as the surface emittance at 8.5-□m decreases. While a relatively small effect, multiple scattering was included in radiative transfer simulations of BTD[8.5-11]. As with any IR technique, BTD[8.5-11] can be used for both daytime and nighttime retrievals. The operational MODIS algorithm relies primarily on brightness temperatures at 8.5 and 11 μm. For midlevel clouds having a cloud-top temperature between 250K and 270K (which are prevalent in both the northern hemisphere and southern hemisphere storm tracks), interpretation of the MODIS measured BTD[8.5-11] values is sometimes problematic and additional information is sometimes needed.

13.3.3 Atmospheric Profiles

The MODIS Atmospheric Profiles product (MOD07) consists of several parameters: they are total-ozone burden, atmospheric stability, temperature and moisture profiles, and atmospheric water vapor. All of these parameters are produced day and night for Level 2 at 5 × 5 1-km pixel resolution when at least 5 FOVs are cloud free. The MODIS total-ozone burden is an estimate of the total-column tropospheric and stratospheric ozone content. The MODIS atmospheric stability consists of three daily Level 2 atmospheric stability indices. The Total Totals (TT), the Lifted Index (LI), and the K index (K) are each computed using the infrared temperature- and moisture-profile data, also derived as part of MOD07. The MODIS temperature and moisture profiles are produced at 20 vertical levels. A statistical regression algorithm based on the infrared radiative transfer equation in a cloudless sky is used. The MODIS atmospheric water-vapor product is an estimate of the total tropospheric column water vapor made from integrated MODIS infrared retrievals of atmospheric moisture profiles in clear scenes.

Temperature and moisture profile retrieval algorithms require calibrated, navigated, and co-registered 1-km FOV radiances from MODIS bands with wavelengths between 4.47 μm (band 24), and 14.24 μm (band 36). The MODIS cloud-mask product (MOD35) is used for cloud screening. The algorithm requires NCEP model analysis of surface pressure. Atmospheric water vapor, or precipitable water, is determined by integrating the moisture profile through the atmospheric column. Atmospheric stability estimates are derived from the MODIS temperature and moisture retrievals contained in this product. Layer temperature and moisture values are used to estimate the temperature lapse rate of the lower troposphere and the low-level moisture concentration.

The atmospheric profiles (MOD07) refer to statistical retrievals of atmospheric temperature and moisture layers, total precipitable water, total column ozone, and stability indices. While MODIS is not per se a sounding instrument, the information content of the high spatial resolution infrared

multi-spectral radiance observations can improve upon a priori definition of atmospheric state by providing better delineation of horizontal gradients. The MODIS clear sky retrievals are performed over land and ocean for both day and night when at least 20% of the radiances measured within a 5x5 field of view area (approximately 5km resolution) are cloud free. The retrieval methods employed here are partly based on the work of the International ATOVS Processing Package (IAPP) (Li et al. 2000) and the Geostationary Operational Environmental Satellite (GOES) sounder algorithms (Ma et al. 1999; Li and Huang 1999; Li et al 2001).

The operational MODIS atmospheric profile algorithm uses 12 infrared channels with wavelengths between 4.465 μm (band 24) and 14.235 μm (band 36). Surface emissivity effects in the short wave infrared bands are mitigated by regressing against band differences (e.g., instead of BT(4.5 μm) and BT(4.4 μm) we use the difference, BT(4.5 μm) - BT(4.4 μm) in the regression, where BT represents brightness temperature). An extension of the NOAA-88 data set containing more than 8400 global radiosonde profiles of temperature, moisture, and ozone is used to determine the regression coefficients. MODIS infrared band radiances are calculated from the radiosonde observations of the atmospheric state, and the regression coefficients are generated from these calculated radiances/atmospheric profile pairs. The radiative transfer calculation of the MODIS spectral band radiances is performed using a transmittance model called Pressure layer Fast Algorithm for Atmospheric Transmittances (PFAAST) (Hannon et al. 1996); this model has 101 pressure level vertical coordinates from 0.05 to 1100 hPa. The calculations take into account the satellite zenith angle, absorption by well-mixed gases (including nitrogen, oxygen, and carbon dioxide), water vapor (including the water vapor continuum), and ozone. In addition, MODIS instrument noise is added into the calculated spectral band radiances.

To perform the retrieval, the regression coefficients are applied to the actual MODIS measurements to obtain the estimated atmospheric profiles, the integration of which yields the total precipitable water (TPW) or total column ozone. The advantage of this approach is that it does not need MODIS radiances collocated in time and space with atmospheric profile data, it requires only historical profile observations. To address radiative transfer model uncertainties and residual instrument calibration anomalies, radiance bias adjustments are made in the retrieval algorithm; these are calculated seasonally from MODIS observed clear sky radiance composites and global model atmospheric analyses. A monthly composite of the total precipitable water vapor for May 2002 inferred from the MODIS infrared spectral bands between 4 and 14.5 μm is shown in Figure 13.10.

13.3.4 Aerosol Properties

Aerosols are one of the greatest sources of uncertainty in climate modeling. Aerosols modify cloud microphysics by acting as cloud condensation nuclei (CCN), and, as a result, impact cloud radiative properties and climate. Aerosols scatter back to space and absorb solar radiation. The MODIS aerosol product is used to study aerosol climatology, sources and sinks of specific aerosol types (e.g., sulfates and biomass burning aerosol), interaction of aerosols with clouds, the hydrological cycle and atmospheric dynamics, and atmospheric corrections of remotely sensed surface reflectance over the land.

MODIS measures aerosols, which include dust, sea salt, volcanic emissions, smoke from forest fires, and some kinds of pollution, directly affect how much sunlight reaches the earth by scattering and absorbing incoming radiation. Scattering of radiation by light-colored particles tends to cool the Earth's surface, and absorption by dark-colored particles tends to warm the atmosphere. Aerosols can simultaneously cool the surface, but warm the atmosphere. Climatologists have long thought that aerosols' cooling effects outweigh their warming effects. They know, for example, that a volcanic eruption can spew dust, ash, and sulfur dioxide into the upper atmosphere (the stratosphere). The light-colored sulfuric acid particles that form in the stratosphere as a result of the eruption can produce a cooling effect at the surface that can last for years. However, recent studies suggest that soot from fossil fuel and biomass burning may contaminate more aerosols than scientists previously thought and that the warming of the atmosphere by these black-carbon

aerosols might exceed the cooling effect at the Earth's surface. The resulting atmospheric heating could alter global air circulation and rainfall patterns across the world.

In addition to their direct interaction with sunlight, aerosols also influence climate indirectly, by interacting with clouds. When water evaporates from the Earth's surface, it disperses throughout the atmosphere. Without aerosols, water vapor would continue to disperse until it was distributed evenly throughout the atmosphere, but there would be no clouds and no rain. This is because water vapor needs a surface on which to condense, or form liquid droplets. Aerosols provide this surface, serving as a "seed" for attracting condensation.

Increasing concentrations of aerosols may increase condensation by providing more surfaces on which raindrops can form, but clouds formed from manmade aerosols are different from clouds formed from natural ones. Because manmade aerosols are typically smaller and more numerous than natural ones, clouds containing lots of manmade aerosols contain larger numbers of smaller liquid water drops. Clouds with many small drops are brighter than those with larger drops, meaning that they reflect more solar radiation back into space. This increased brightness has a cooling effect, which might be expected to counteract a CO2-induced warming trend. However, small drops often evaporate before they can fall from the sky as rain. One possible outcome of increasing aerosol pollution could be more clouds, but less rain.

Aerosol Properties are provided by MODIS (MOD04). Aerosols must be accounted for during the retrieval of surface and atmospheric parameters. The MODIS aerosol products document one of the most elusive and least understood radiatively active components of the atmosphere by providing information on aerosol optical thickness, aerosol size distribution, and aerosol sources and sinks. The MODIS Aerosol Product (MOD04) monitors the ambient aerosol optical thickness over the oceans globally and over a portion of the continents. Further, the aerosol size distribution is derived over the oceans, and the aerosol type is derived over the continents. Daily Level 2 (MOD04) data are produced at the spatial resolution of a 10 x10 1-km (at nadir) pixel array.

Prior to MODIS, satellite aerosol measurements were limited to reflectance measurements in one (GOES, METEOSAT) or two (AVHRR) channels. There was no real attempt to retrieve aerosol content over land on a global scale. Algorithms had been developed for use only over dark vegetation. The blue channel on MODIS, not present on AVHRR, offers the possibility to extend the derivation of optical thickness over land to additional surfaces. The algorithm uses MODIS bands 1 through 7 and requires prior cloud screening using MODIS data. Over the land, the dynamic aerosol models are derived from ground-based sky measurements and used in the net retrieval process. Over the ocean, three parameters that describe the aerosol loading and size distribution are retrieved. Pre-assumptions on the general structure of the size distribution are required in the inversion of MODIS data, and the volume-size distribution are described with two log-normal modes: a single mode to describe the accumulation mode particles (radius <0.5 μm) and a single coarse mode to describe dust and / or salt particles (radius > 1.0 μm). Figure 13.11 shows the September 2000 composite of the aerosol optical thickness (referenced to 550 nm) over ocean derived from the coarse particle model that uses MODIS bands at 550, 660, 865, 1230, 1640, 2130 nm. The aerosol parameters retrieved are the ratio between the two modes, the spectral optical thickness, and the mean particle size.

The aerosol product (MOD04) is based on different algorithms for the remote sensing of tropospheric aerosol over land (Kaufman et al., 1997) and ocean (Tanre et al., 1997). Both algorithms try to match MODIS observed reflectances to a lookup table of precomputed reflectances for a wide variety of commonly observed aerosol conditions, as summarized by King et al. (1999). Over land, the prime difficulty is separating the reflectance measured by the satellite into an atmospheric part and a land surface part. This difficulty is overcome by estimating the visible surface reflectance from the MODIS-measured reflectance in the shortwave infrared wavelength (2.13 μm) for dark targets, as described by Kaufman et al. (1997). Removing the estimated surface reflectance from the total measured by the satellite, the atmospheric contribution is isolated by using lookup tables to determine the aerosol characteristics and optical thickness in the scene.

Final land products include aerosol optical thickness at 0.47, 0.56, and 0.65 μm at a 10-km spatial resolution. The spectral dependence of the reflectance across the visible wavelengths is then used to obtain a rough estimate of the fine mode (radius < 0.6 μm) fraction of the aerosol optical thickness at 0.56 μm.

The ocean algorithm assumes that the surface reflectance contribution to the total reflectance is small and can be calculated from geometry and assumptions about the sea state. The better-characterized ocean surface permits the use of reflectances at six wavelengths (0.56–2.13 m) in the derivation. Again, the retrieved aerosol products are represented by the best fits between observed reflectance and the lookup table. Ocean products include aerosol optical thickness at 0.47, 0.56, 0.65, 0.86, 1.24, 1.64, and 2.13 μm at a 10-km spatial resolution. Using a wide spectral range over ocean allows the derivation of the effective radius of the particle population, and more accurate determination of fine mode fraction than over land. The aerosol algorithm is applied to cloud free conditions outside the sunglint region (glint angle < 40) and for land surface reflectance at 2.13 μm 0.25 at nadir and 0.4 at slant view directions. The comparison with the lookup table is performed for the average of the 25% to 75% pixels over the ocean and 20% to 50% over the land in order to avoid any undetected nonaerosol contamination. A minimum of ten (12) pixels is required for the analysis in any 10-km region over ocean (land).

13.3.5 Sea Surface Temperature

SST temperature influences ocean productivity. Every three to five years Pacific coast fishermen experience a significantly smaller than average catch around December and January; they named the phenomenon El Niño. Scientists determined that the small catch was related to fluctuations in SST and wind patterns. Normally, winds push the warmer waters of the equatorial Pacific westward, allowing colder, nutrient-rich water from deeper layers of the ocean to well up to the surface. The influx of nutrients supports a lush phytoplankton population, which in turn supports the fish. During an El Niño event, the easterly winds die off, and warm water replaces the cold, nutrient-rich water, causing populations to decline. El Niño events also radically alter rainfall and drought patterns in North America, Africa, South America, Australia, India and Indonesia. Accurate global measurements of SST will help scientists understand and predict short-term climate events like El Niño as well as long-term climate change.

The surface temperature can be expressed in terms of the observed clear sky infrared window BT and a water vapour correction that ranges from a few tenths of a degree Kelvin in very cold and dry atmospheres to nearly 10 K in very warm and moist atmospheres for 11 μm window observations. The corresponding corrections for the 4 μm window are about half as large. Corrections are estimated using measurements in two windows of varying water vapor sensitivity and extrapolating to a moisture free measurement; both MODIS and VIIRS have 11 and 12 μm as well as 3.7 and 4 μm split windows (the latter pair can only be reliably used at night as reflected solar radiation interferes during the day). Figure 13.12 shows a composite of MODIS night SSTs for 1-7 September 2000; the coverage and detail in the tropical waters is especially noteworthy.

13.3.6 Hot Spot Detection

Some of the most easily recognizable changes are occurring on land. Human-induced changes such as deforestation, urbanization, and hydroelectric and irrigation projects combine with the Earth's existing cycles of fire, erosion, and floods to change our landscape. While we can often see these changes happening on a local scale, it is impossible to assess global effects through fieldwork alone. With its near-daily coverage of the Earth's surface, MODIS provides comprehensive measurements that scientists and land managers need to make informed decisions about managing Earth's natural resources from season to season, year to year, and decade to decade.

Information on the occurrence of fires on the land surface is relevant to climate change, since fire changes the surface cover type and releases gases and particulate matter into the atmosphere,

affecting ecosystems and atmospheric chemistry. Fire is also a hazard and satellite derived fire information can be used for improved fire and forest management. Identification of active volcanoes is also important because of the geophysical consequences they have on the Earth's atmosphere, including ozone destruction and the lowering of the global temperature.

The MODIS fire and thermal anomalies products contain information unique to understanding the timing and distribution of fires and characteristics such as the energy emitted from the fire and is available for both day and night periods. Temporal composites include an eight-day and monthly day and night fire occurrence aggregation and a summary of the number of fires in classes related to the strength of the fire. A one-day example of global fire coverage is shown in Figure 13.13.

13.4 MODIS and Climate Investigations

MODIS is a key instrument aboard the Terra (EOS AM) and Aqua (EOS PM) satellites. Terra's orbit around the Earth is timed so that it passes from north to south across the equator in the morning, while Aqua passes south to north over the equator in the afternoon. Terra MODIS and Aqua MODIS are viewing the entire Earth's surface every 1 to 2 days, acquiring data in 36 spectral bands, or groups of wavelengths. The MODIS spectral selection is based on heritage sensors such as the Advanced Very High Resolution Radiometer (AVHRR), used for meteorology and monitoring sea surface temperature, sea ice, and vegetation; the Coastal Zone Color Scanner (CZCS) and the Sea-viewing Wide Field of View Sensor (SeaWiFS), used to monitor ocean biological activity; Landsat, used to monitor terrestrial conditions; and NOAA’s High Resolution Infrared Radiation Sounder (HIRS), used to observe atmospheric conditions. By extending these data sets, MODIS promotes the continuity of data collection essential for understanding both long- and short-term change in the global environment. These data will improve our understanding of global dynamics and processes occurring on the land, in the oceans, and in the lower atmosphere. MODIS is playing a vital role in the development of validated, global, interactive Earth system models able to predict global change accurately enough to assist policy makers in making sound decisions concerning the protection of our environment.

Table 13.1: MODIS Channel Number, Wavelength (μm), and Primary Application

Reflective Bands		
1,2	0.645, 0.865	land/cld boundaries
3,4	0.470, 0.555	land/cld properties
5-7	1.24, 1.64, 2.13	land/cld properties
8-10	0.415, 0.443, 0.490	ocean color/chlorophyll
11-13	0.531, 0.565, 0.653	ocean color/chlorophyll
14-16	0.681, 0.75, 0.865	ocean color/chlorophyll
17-19	0.905, 0.936, 0.940	atm water vapor
26	1.375	cirrus clouds
Emissive Bands		
20-23	3.750(2), 3.959, 4.050	sfc/cld temperature
24,25	4.465, 4.515	atm temperature
27,28	6.715, 7.325	water vapor
29	8.55	sfc/cld temperature
30	9.73	ozone
31,32	11.03, 12.02	sfc/cld temperature
33-36	13.335, 13.635, 13.935, 14.235	cld top properties

Table 13.2: Summary of the MODIS data products

Cloud mask at 250 m and 1000 m resolution during the day and 1000 m resolution at night.
Aerosol concentration and optical properties at 10 km resolution during the day.
Cloud properties (optical thickness, effective particle radius, thermodynamic phase, cloud top altitude, cloud top temperature, cirrus reflectance) at 1-5 km resolution during the day
and 5 km resolution at night.
Total precipitable water at 1-5 km resolution during the day and 5 km resolution at night.
Atmospheric temperature and water vapor profiles.
Vegetation and land-surface cover, conditions, and productivity, defined as
- Surface reflectance at 250 m, 500 m, and 1 km resolution
- Vegetation indices corrected for atmospheric effects, soil, polarization, and directional effects at 250 m and 500 m resolution
- Land cover
  * Global, 1-km IGBP Land Cover Classification
  * Vegetation continuous fields, sub-pixel land cover components
  * Vegetative cover conversion, global land cover change alarm at 250 m
  * Net primary productivity, leaf area index, and intercepted photosynthetically active radiation at 1-km resolution

Gridded atmosphere products at 10° resolution globally for daily, eight-days and monthly periods.
Fire and thermal anomalies at 1-km resolution
Snow and sea-ice cover and reflectance at 500-m and 5-km Climate Modeling Grid
Surface temperature with 1-km resolution, day and night, skin and bulk, with absolute accuracy
goals of 0.3°C - 0.5°C over oceans and 1°C over land; Ocean temperature available daily
at 1 km (granules), and global daily, weekly, and monthly at 4.6 km, 36 km, and 1°.
Ocean bio-optical properties, including water-leaving radiances at daily 1-km resolution, and productivity at weekly, 4.6 km, 36 km and 1° resolution
- Water-leaving radiance corrected for atmospheric, polarization, and directional effects
- Chlorophyll-a concentration from 0.01 to 50 mg/m-2
- Chlorophyll-a fluorescence and fluorescence efficiency
- Coccolithophore pigment concentration and calcite concentration

- Suspended sediment concentration
- Phytoplankton spectral absorption
- Dissolved organic matter absorption
- Primary productivity weekly indices

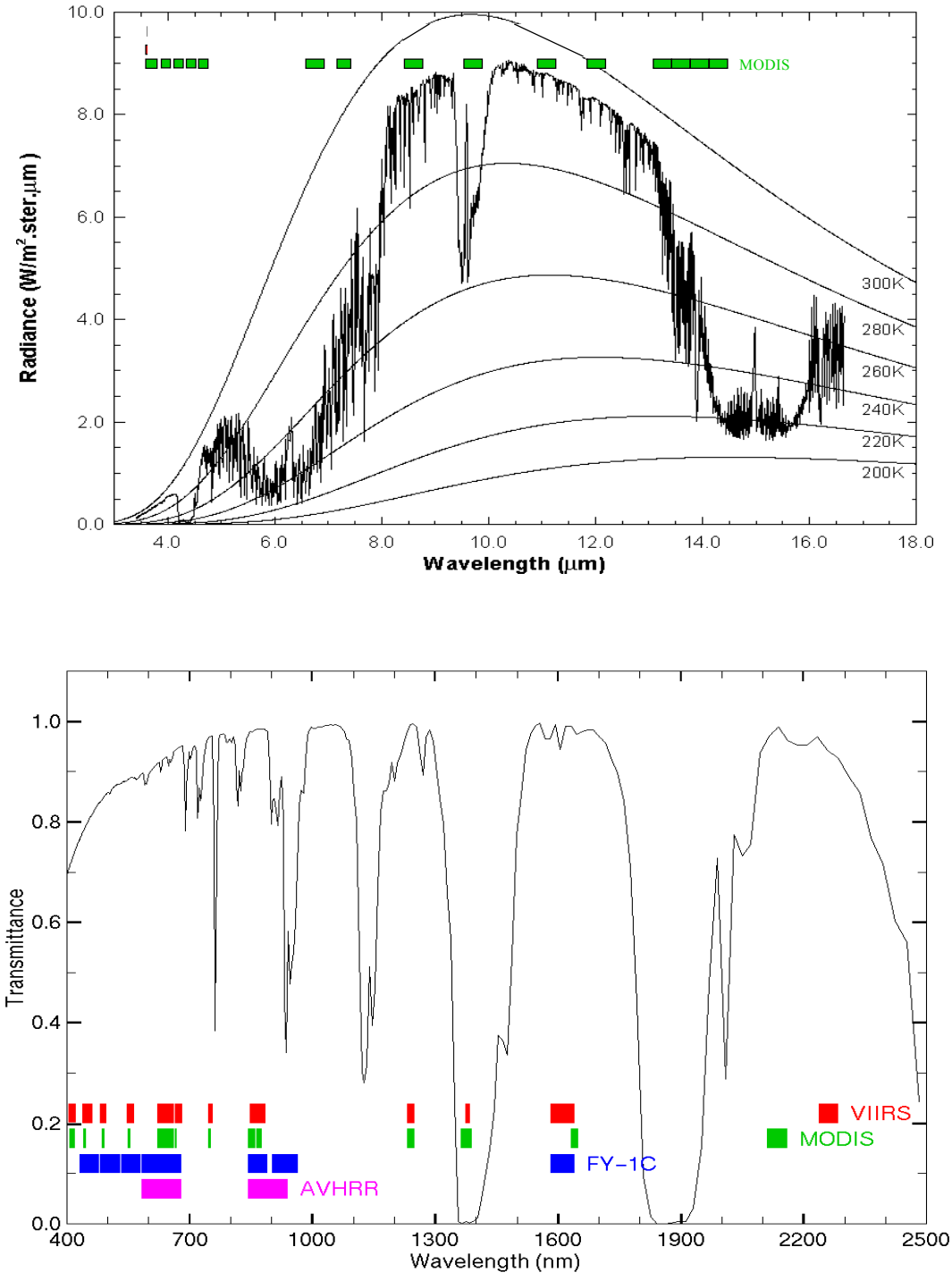

Figure 13.1: MODIS emissive bands superimposed on a high resolution earth atmosphere

emission spectra with Planck function curves at various temperatures superimposed (top) and MODIS reflective spectral bands superimposed on the earth reflection spectra (bottom).

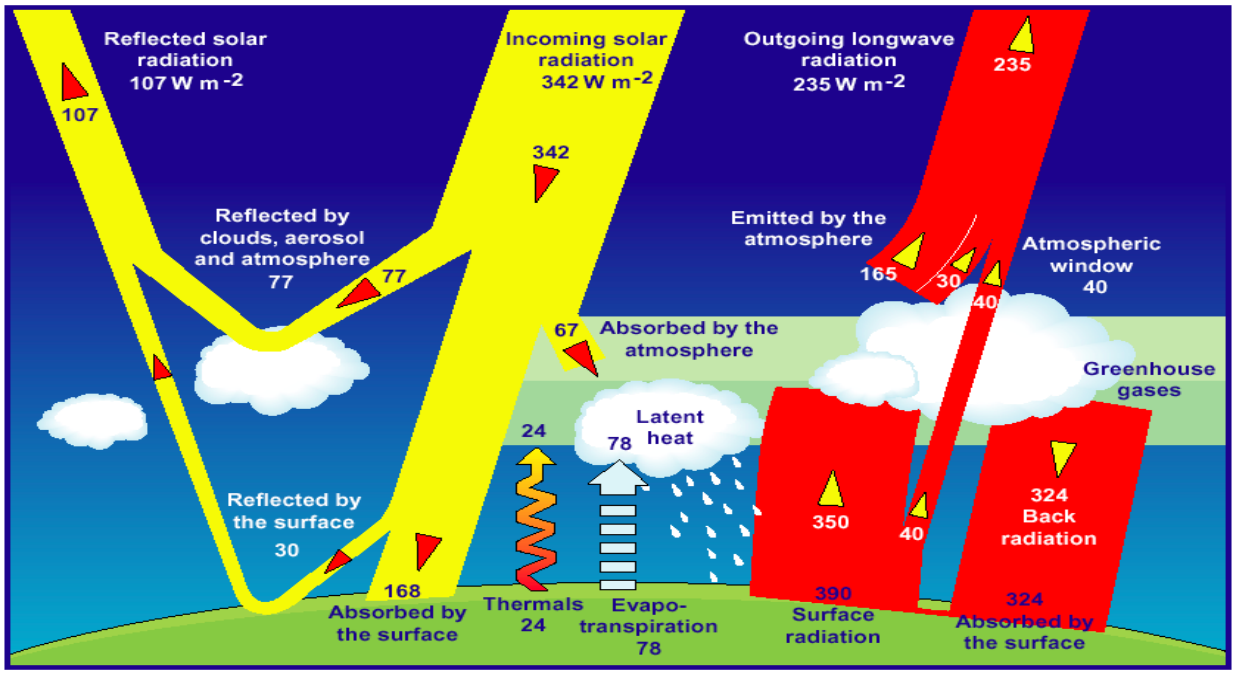

Figure 13.2: Climate system energy balance with role of clouds, evaporation, and other radiative processes indicated in watt per meters squared.

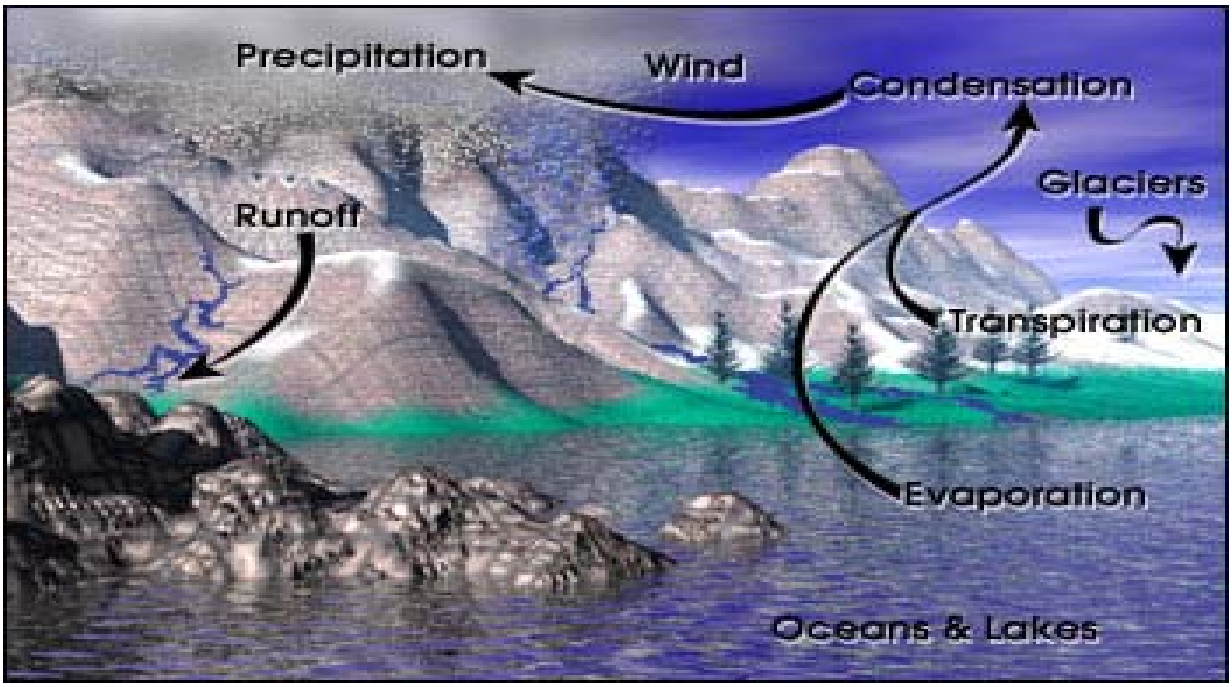

Figure 13.3: In the hydrologic cycle, individual water molecules travel between the oceans, water vapor in the atmosphere, water and ice on the land, and underground water.

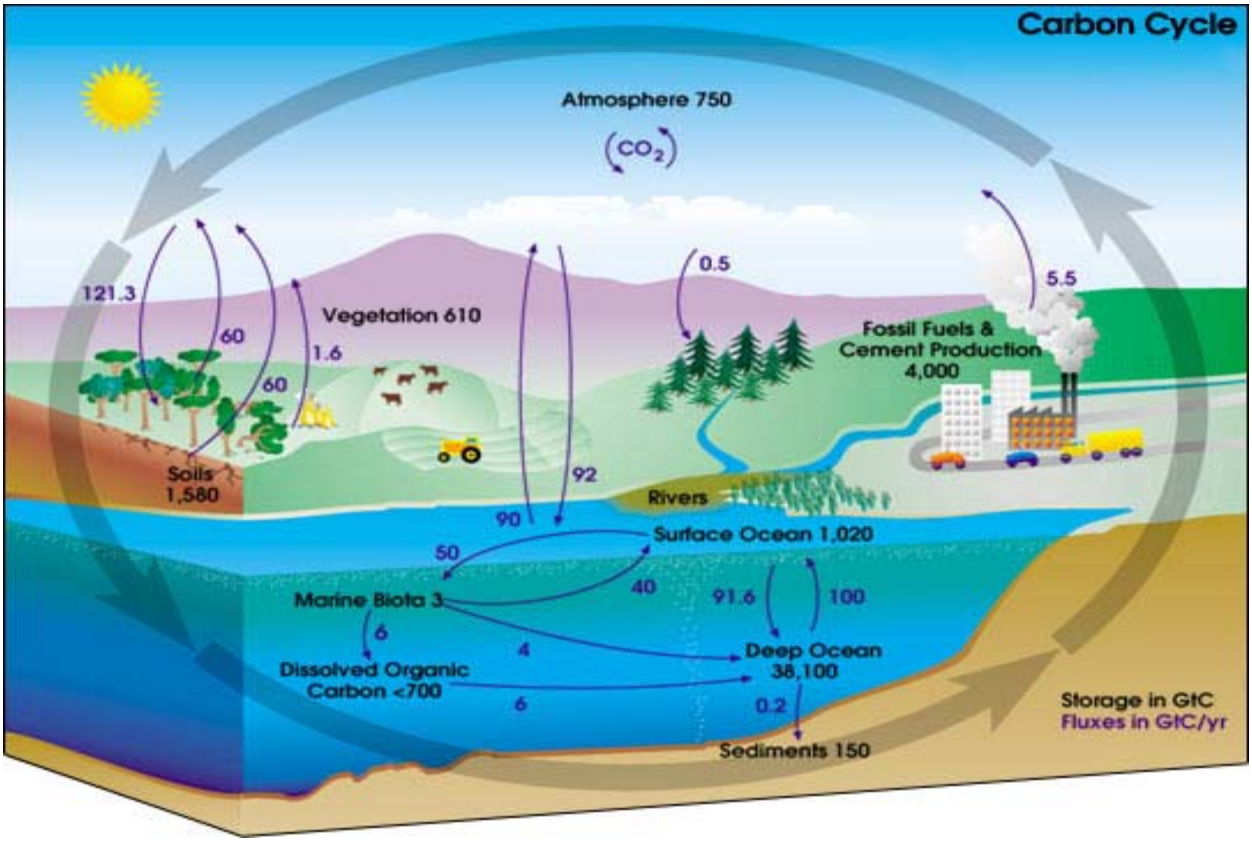

Figure 13.4: The carbon cycle illustrated with total amounts of stored carbon in black, and annual carbon fluxes in purple. In any given year, tens of billions of tons of carbon move between the atmosphere, hydrosphere, and geosphere. Human activities add about 5.5 billion tons per year of carbon dioxide to the atmosphere.

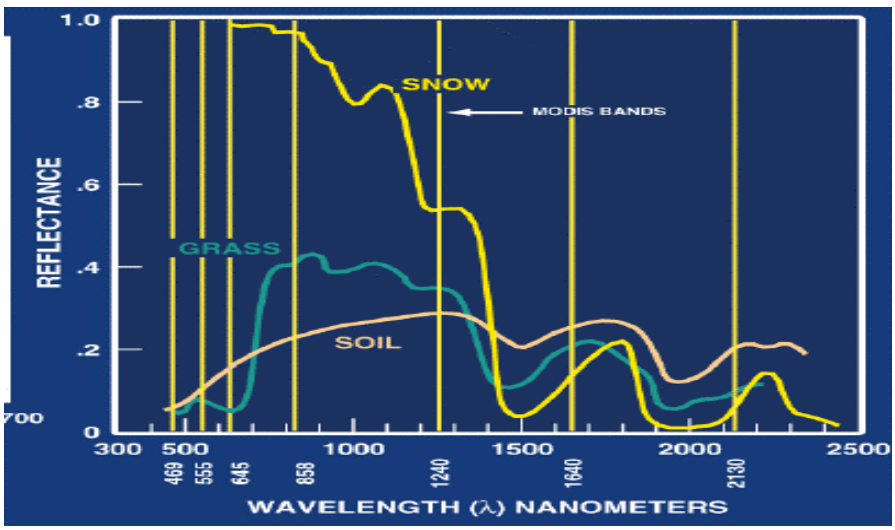

Figure 13.5a: Spectral reflectance for various surfaces between 300 and 2500 nanometers.

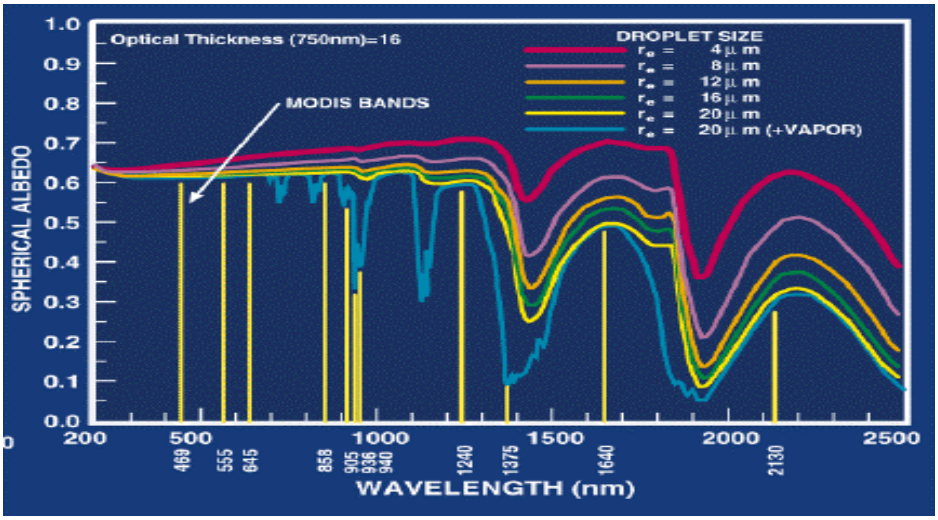

Figure 13.5b: Spectral changes in spherical albedo between 200 and 2500 nanometers for water clouds with droplet sizes between 4 and 20 microns.

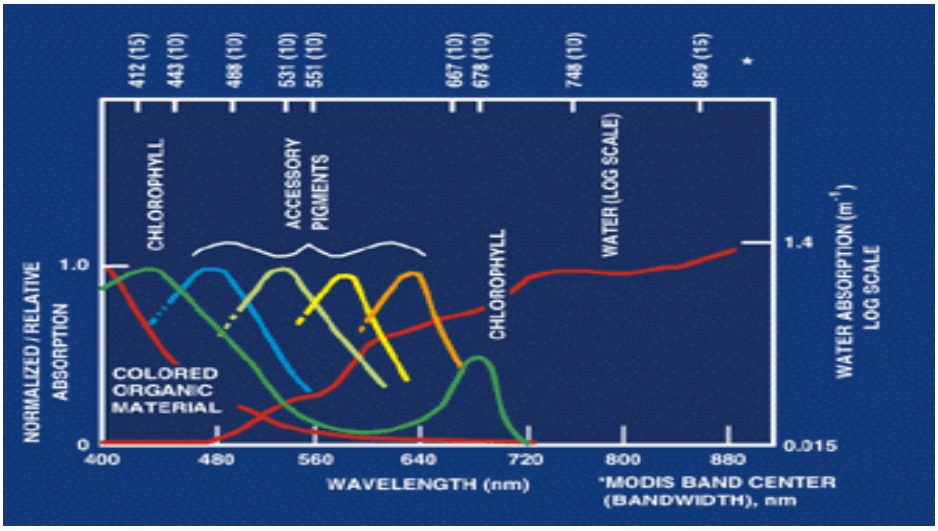

Figure 13.5c: Spectral changes in normalized relative absorption between 400 and 880 nanometers for chlorophyll and various associated pigments.

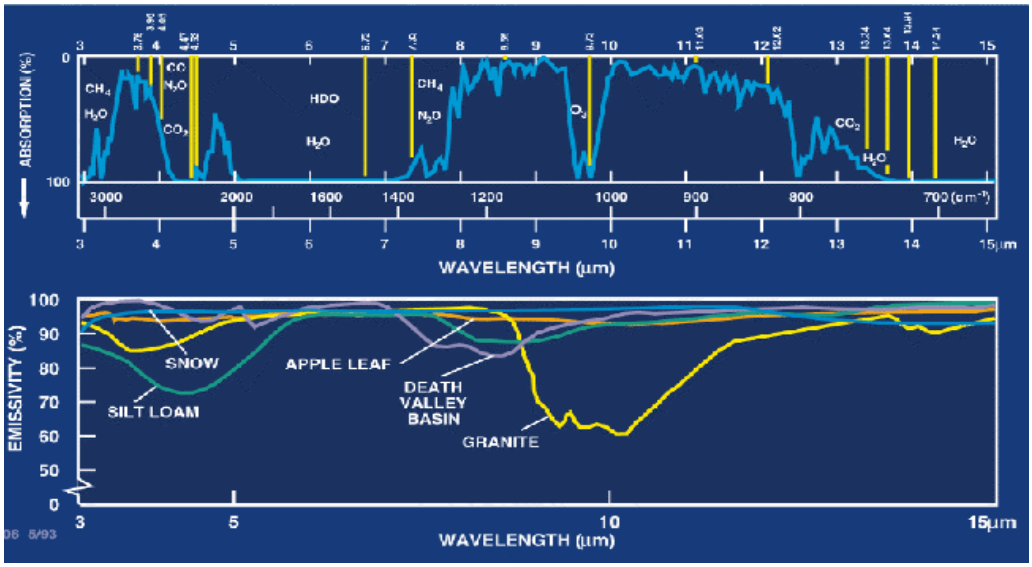

Figure 13.5d: Atmospheric absorption (top) and surface emissivity (bottom) between 3 and 15 um.

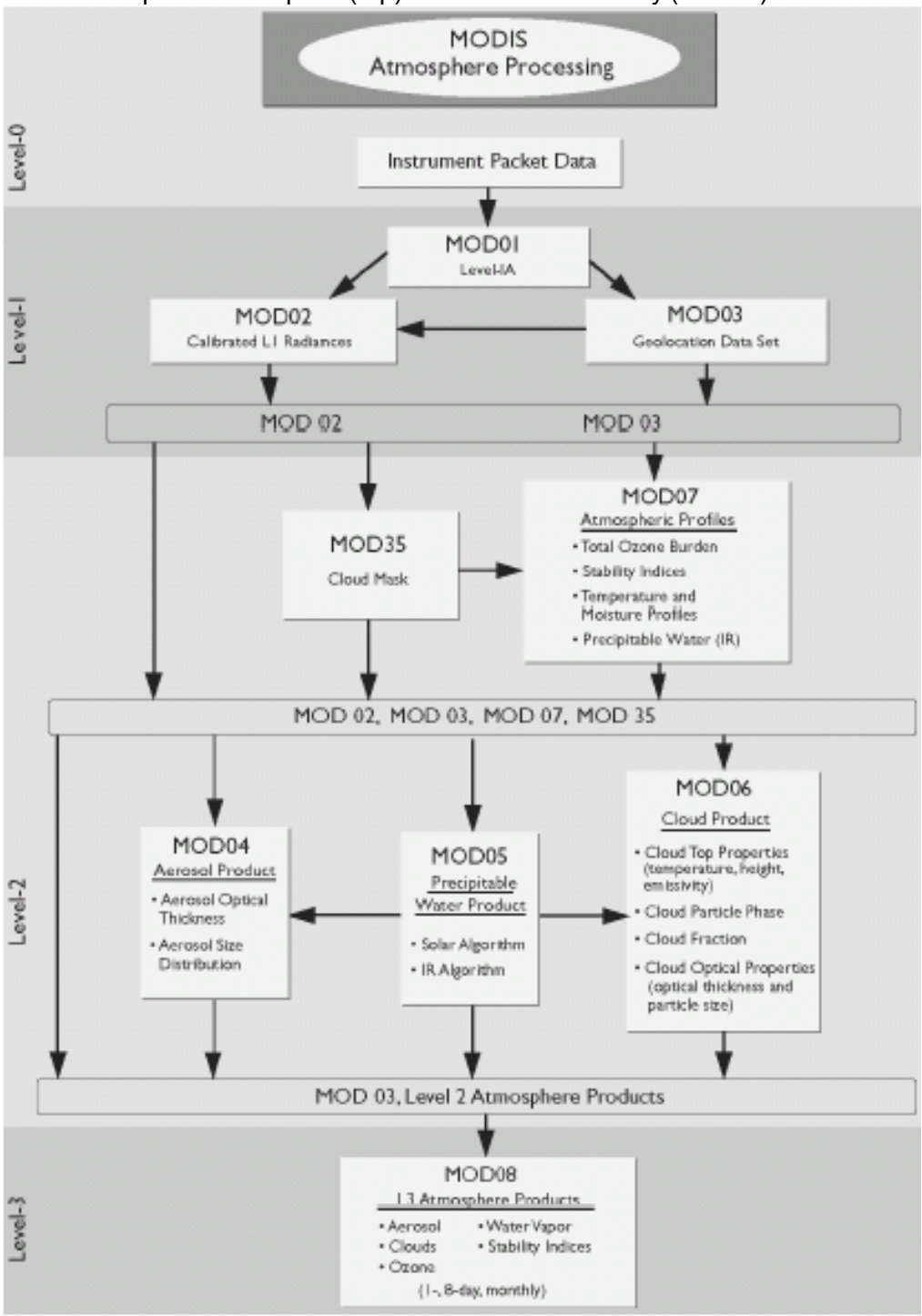

Figure 13.6: MODIS Atmospheric Processing schema from level 0 (raw instrument data) to level 1 (calibrated earth located radiances) to level 2 (5x5 field of view derived atmospheric products) to level 3 (time composited global product fields in even interval lat-lon grid boxes). Adapted from the EOS Data Products Handbook (Parkinson and Greenstone, 2000)

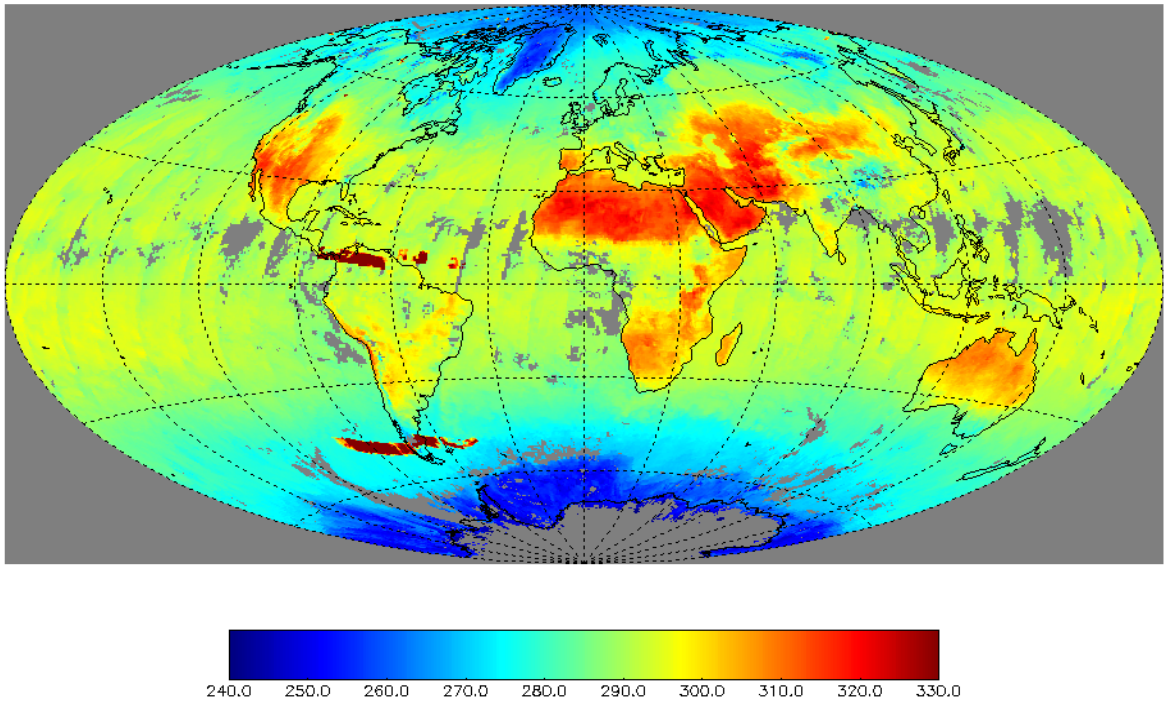

Figure 13.7. Composite clear-sky MODIS 11 μm brightness temperature for 5-8 September 2000 (red-315 K yellow-295 K, blue-265 K)

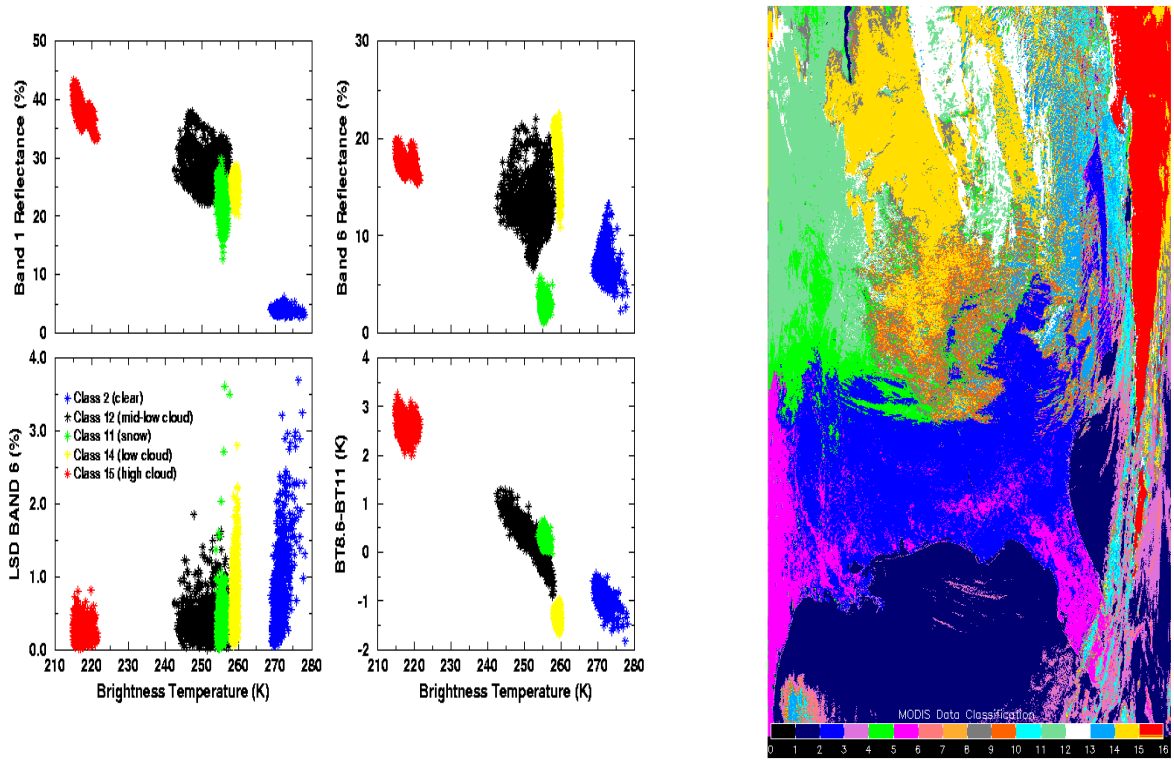

Figure 13.8: (left) Scatter plots of MODIS 0.645 μm band 1 (upper left panel), 1.6 μm band 6 (upper right panel), Local Standard Deviation (LSD) of band 6 (lower left panel), 8.6 minus 11 μm (lower right panel) and versus 11 μm brightness temperature for clear (blue) snow (green), low clouds (yellow), mid-low clouds (black), high clouds (red). (right) Cloud classification for eastern United States on 17 December 2000 at 1640 UTC.

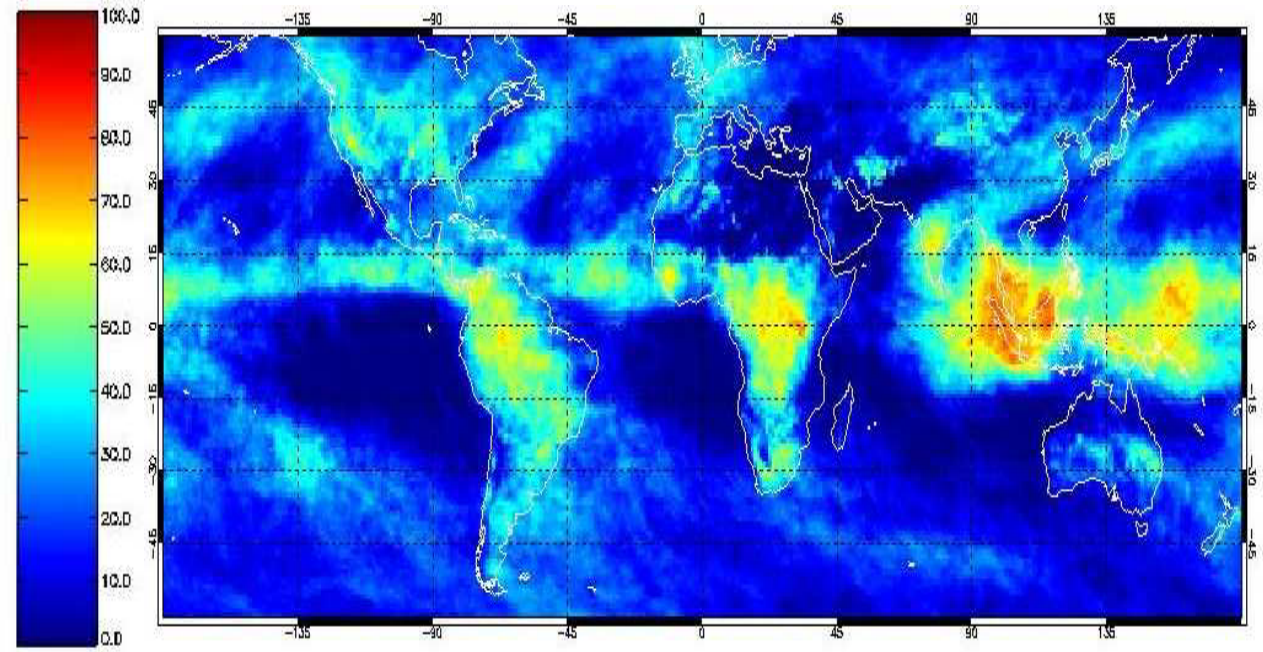

Figure 13.9: Monthly composite of the percentage of observations with high clouds (above 400 hPa)) for October 2001 inferred from the MODIS CO2 sensitive infrared spectral bands between 11 and 14.5 microns.

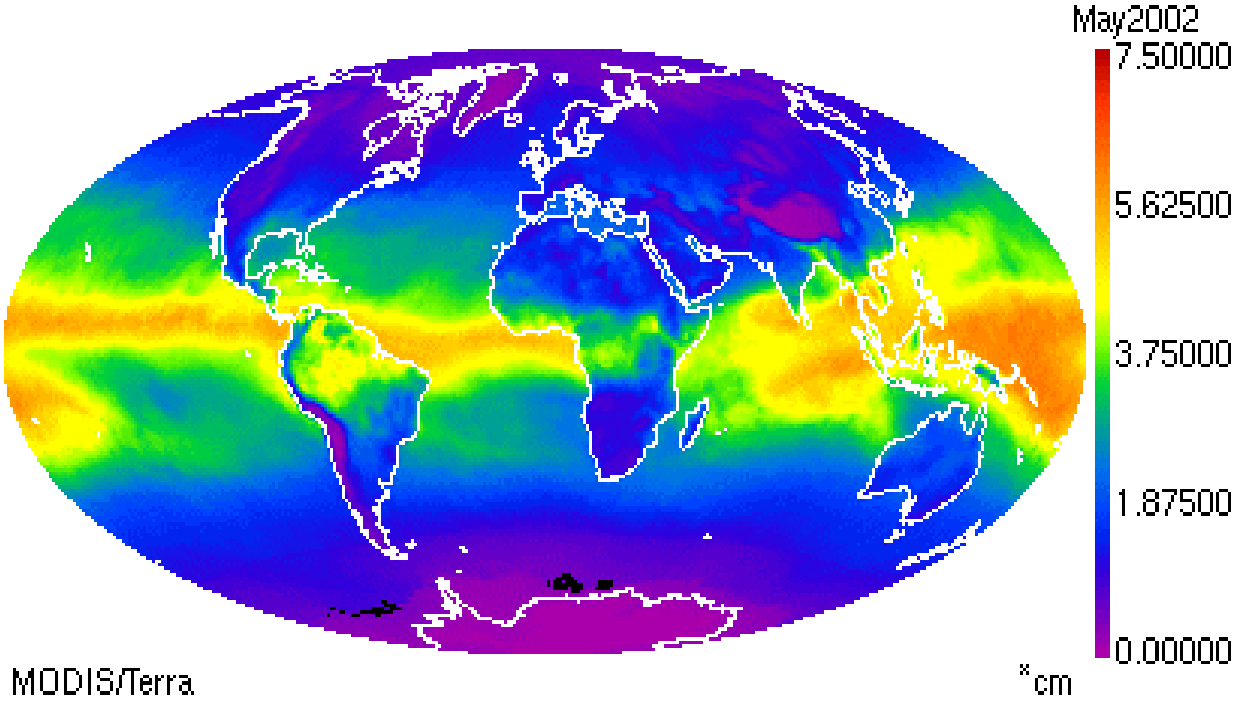

Figure 13.10: Monthly composite of the total precipitable water vapor in cm for May 2002 inferred from the MODIS infrared spectral bands between 4 and 14.5 microns.

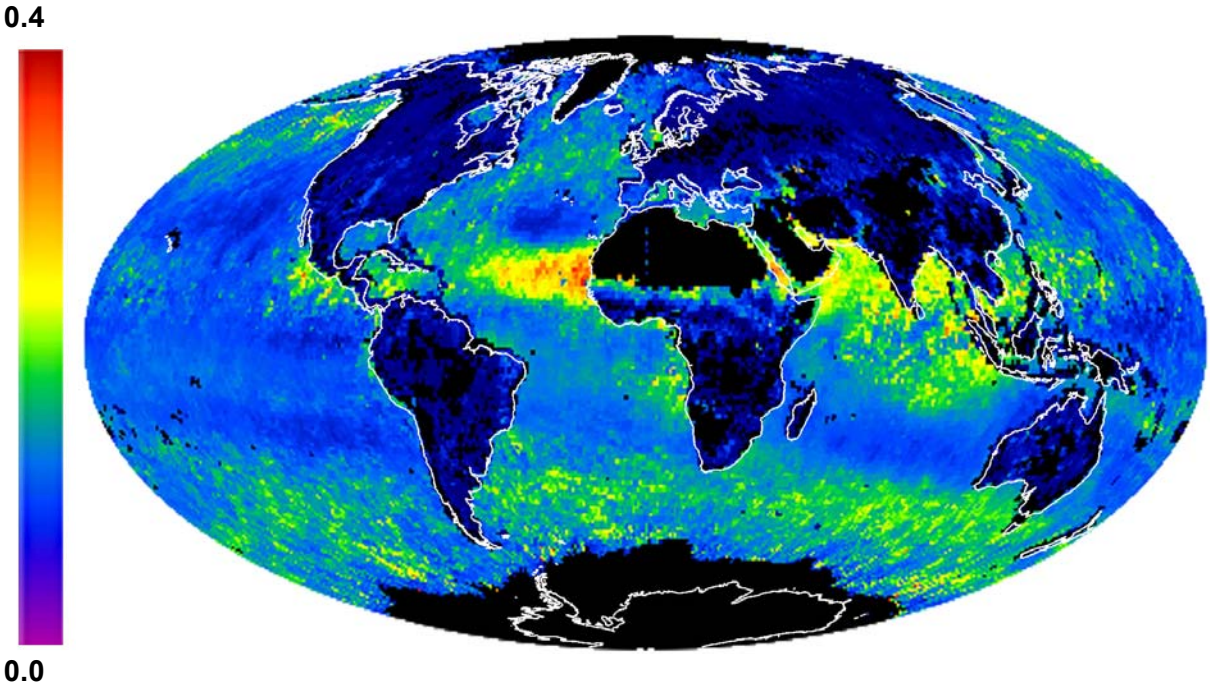

Figure 13.11: Monthly composite of the aerosol optical thickness for September 2000 (referenced to 550 nm) over ocean derived from the coarse particle model that uses MODIS bands at 550, 660, 865, 1230, 1640, 2130 nm.

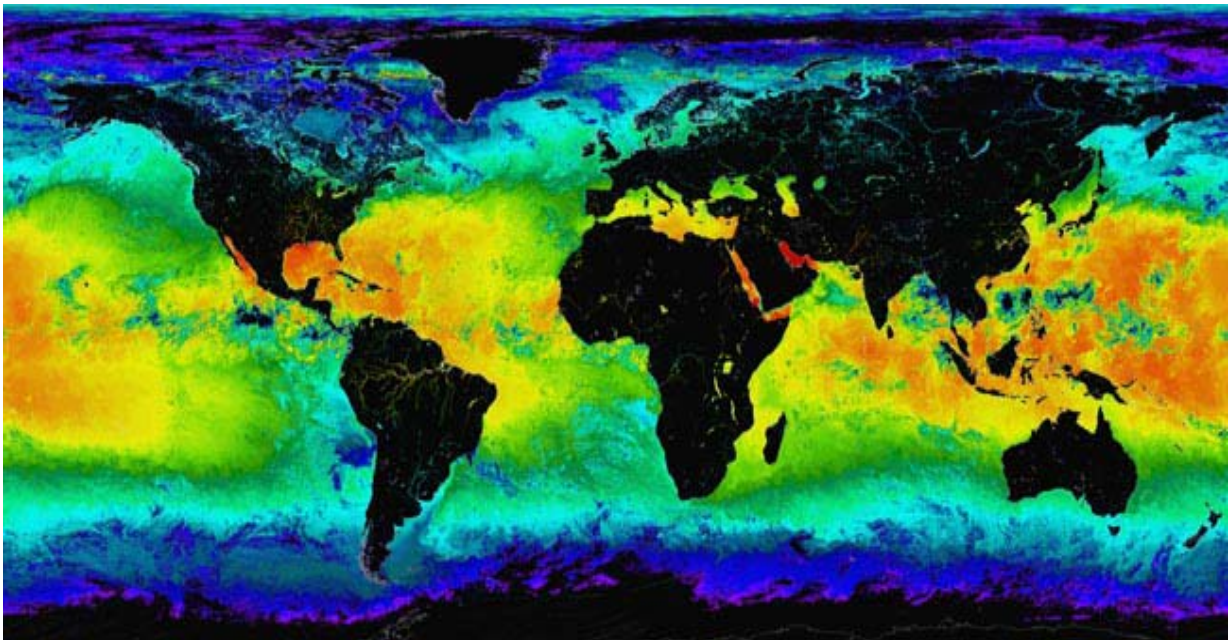

Figure 13.12: Composite of MODIS night SSTs for 1-7 September 2000 estimated using the 3.7 and 4 μm split window (generated at the University of Miami).

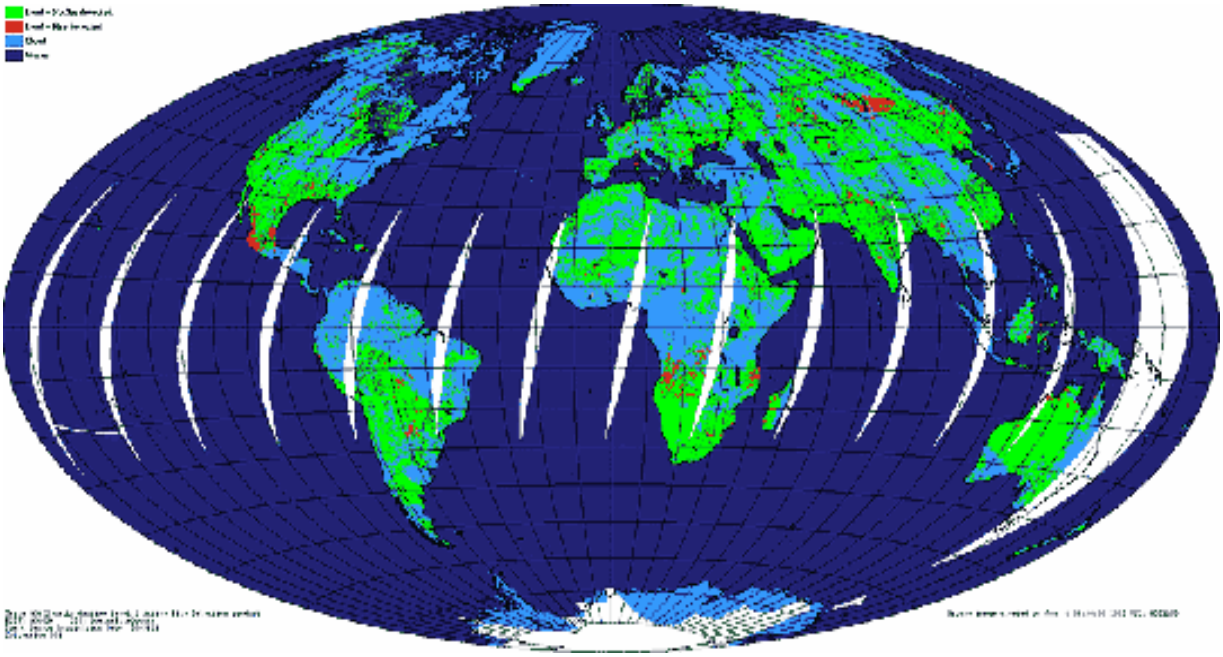

Figure 13.13: Daily, coarse-resolution (5 and 20 km) global summary fire imagery indicating areas in which active fires were detected. This product is generated using the MODIS 4 and 11micron channels as well as the visible channels (daytime only). This example at greatly reduced resolution, shows fires colored red, water in dark blue, clear land in green, clouds in cyan, and missing data in white.

References

For Cloud Properties

Ackerman, S. A., K. I. Strabala, W. P. Menzel, R. A. Frey, C. C. Moeller, and L. I. Gumley, 1998: Discriminating clear-sky from clouds with MODIS. J. Geophys. Res., 103, D24 , 32141-32158.

Baum, B. A. and B. A. Wielicki: Cirrus cloud retrieval using infrared sounding data: Multilevel cloud errors. *J. Appl. Meteor.*, *33*, No. 1, 107-117, 1994.

Baum, B. A., et al., Remote sensing of cloud properties using MODIS airborne simulator imagery during SUCCESS, 1, Data and Models, *J. Geophys. Res.*, *105*, 11,767-11,780, 2000a.

Baum, B. A., et al., Remote sensing of cloud properties using MODIS airborne simulator imagery during SUCCESS, 2, Cloud thermodynamic phase, *J. Geophys. Res.*, *105*, 11,781-11,792, 2000b.

King, M. D., Y. J. Kaufman, W. P. Menzel, and D. Tanre, 1992: Remote Sensing of Cloud, Aerosol and Water Vapor Properties from the Moderate Resolution Imaging Spectrometer (MODIS). IEEE Trans. and Geoscience and Remote Sensing, 30, 2-27.

King, M. D., W. P. Menzel, Y. J. Kaufman, D. Tanré, B. C. Gao, S. Platnick, S. A. Ackerman, L. Remer, R. Pincus, and P. A. Hubanks, 2003: Cloud and aerosol properties, precipitable water, and profiles of temperature and humidity from MODIS. IEEE Trans. Geosci. Remote Sens., **41**, 442-458.

Menzel, W. P., W. L. Smith, and T. R. Stewart, Improved cloud motion wind vector and altitude assignment using VAS, *J. Appl. Meteorol*., 22, 377-384, 1983.

Platnick, S., M. D. King, S. A. Ackerman, W. P. Menzel, B. A. Baum, J. C. Riédi, and R. A. Frey, 2003. The MODIS cloud products: Algorithms and examples from Terra," *IEEE Trans. Geosci. Remote Sensing*, vol. 41, pp. 459-473.

Strabala, K. I., S. A. Ackerman and W. P. Menzel, Cloud properties inferred from 8-12 □m data, *J. Appl. Meteor.*, *2*, 212-229, 1994.

Wielicki, B. A., and J. A. Coakley, Jr., Cloud retrieval using infrared sounder data: Error analysis. *J. Appl. Meteor. 20*, 157-169, 1981.

Wylie, D. P., and W. P. Menzel, Eight years of high cloud statistics using HIRS, *Journal of Climate*, *12*, 170-184, 1999.

For Atmospheric Profiles

Hannon, S., L. L. Strow, and W. W. McMillan, 1996: Atmospheric Infrared Fast Transmittance Models: A Comparison of Two Approaches. Proceeding of SPIE conference 2830, Optical Spectroscopic Techniques and Instrumentation for Atmospheric and Space Research II.

Li, J., and H.-L. Huang, 1999: Retrieval of atmospheric profiles from satellite sounder measurements by use of the discrepancy principle, *Appl. Optics*, Vol. 38, No. 6, 916-923.

Li, J., C. C. Schmidt, J. P. Nelson, T. J. Schmit, and W. P. Menzel, 2001: Estimation of total ozone from GOES sounder radiances with high temporal resolution. *Journal of Atmospheric and Oceanic Technology,* 157 – 168.

Li, J., W. Wolf, W. P. Menzel, W. Zhang, H.-L. Huang, and T. H. Achtor, 2000: Global soundings of the atmosphere from ATOVS measurements: The algorithm and validation, *J. Appl. Meteorol.,* 39: 1248 – 1268.

Ma, X. L., Schmit, T. J. and W. L. Smith, 1999: A non-linear physical retrieval algorithm – its application to the GOES-8/9 sounder. *J. Appl. Meteor*. 38, 501-513.

Menzel, W. P., and J. F. W. Purdom, 1994: Introducing GOES-I: The first of a new generation of geostationary operational environmental satellites. *Bull. Amer. Meteor. Soc.*, **75**, 757-781.

Menzel, W. P., F. C. Holt, T. J. Schmit, R. M. Aune, A. J. Schreiner, G. S. Wade, and D. G. Gray, 1998. Application of the GOES-8/9 soundings to weather forecasting and nowcasting. *Bull. Amer. Meteor. Soc*., **79**, 2059-2077.

For Aerosol Properties

S. A. Ackerman, K. I. Strabala,W. P. Menzel, R. A. Frey, C. C. Moeller,and L. E. Gumley, 1998. Discriminating clear sky from clouds with MODIS. *J. Geophys. Res.*, vol. 103, pp. 32 141–32 157

W. L. Barnes, T. S. Pagano, and V. V. Salomonson, 1998. Prelaunch characteristics of the Moderate Resolution Imaging Spectroradiometer (MODIS) on EOS-AM1. *IEEE Trans. Geosci. Remote Sensing*, vol. 36, pp. 1088–1100.

D. A. Chu, Y. J. Kaufman, C. Ichoku, L. A. Remer, D. Tanré, and B. N. Holben, 2002. Validation of MODIS aerosol optical depth retrieval over land. *Geophys. Res. Lett.* [Online], vol (12).
Available: DOI 10.1029/2001GL013205.

B. N. Holben, T. F. Eck, I. Slutsker, D. Tanré, J. P. Buis, A. Setzer, E. Vermote, J. A. Reagan, Y.
J. Kaufman, T. Nakajima, F. Lavenu, I. Jankowiak, and A. Smirnov, 1998. AERONET—A federated instrument network and data archive for aerosol characterization," *Remote Sens. Environ.*,vol. 66, pp. 1–16.

Y. J. Kaufman, D. Tanré, L. A. Remer, E. F. Vermote, A. Chu, and B. N. Holben, 1997. Operational remote sensing of tropospheric aerosol over land from EOS moderate resolution imaging spectroradiometer," *J. Geophys. Res.*, vol. 102, pp. 17051–17 067.

M. D. King, Y. J. Kaufman, W. P. Menzel, and D. Tanré, 1992. Remote sensing of cloud, aerosol, and water vapor properties from the Moderate Resolution Imaging Spectrometer
(MODIS)," *IEEE Trans. Geosci. Remote Sensing*, vol. 30, pp. 2–27.

C. L. Parkinson and R. Greenstone, 2000. EOS Data Products Handbook. NASA Goddard Space Flight Center, Greenbelt, MD. [Online] eospso.gsfc.nasa.gov. NP-2000-5-055-GSFC.

L. A. Remer, Y. J. Kaufman, and B. N. Holben, 1999. Interannual variation of ambient aerosol characteristics on the east coast of the United States. *J. Geophys. Res.*, vol. 104, pp. 2223–2232.

L. A. Remer, D. Tanré, Y. J. Kaufman, C. Ichoku, S. Mattoo, R. Levy, D. A. Chu, B. N. Holben,

O. Dubovik, A. Smirnov, J. V. Martins, R. R. Li, and Z. Ahmad, 2002. Validation of MODIS aerosol retrieval over ocean. *Geophys. Res. Lett.* [Online], vol (12). Available: DOI 10.1029/2001GL013204.

D. Tanré, Y. J. Kaufman, M. Herman, and S. Mattoo, 1997. Remote sensing of aerosol properties over oceans using the MODIS/EOS spectral radiances. *J. Geophys. Res.*, vol. 102, pp. 16 971–16988.

For fire detection

Kaufman, Y.J., C. O. Justice, L. P. Flynn, J. D. Kendall, E. M. Prins, L. Giglio, D. E. Ward, W. P. Menzel, and A. W. Setzer, 1998: Potential global fire monitoring from EOS-MODIS. J. Geophys. Res., 103, D24, 32215-32238.